JOURNAL OF CATALYSIS 107, 296–306 (1987)

Alkylation of Toluene with Methanol on Commercial X Zeolite in Different Alkali Cation Forms

J. ENGELHARDT, J. SZANYI, AND J. VALYON

Central Research Institute for Chemistry of the Hungarian Academy of Sciences, P.O. Box 17, H-1525 Budapest, Hungary

Received January 20, 1986; revised April 7, 1987

Catalytic alkylation of toluene with methanol was studied at atmospheric pressure, 698 K, and toluene/methanol = 5 mol/mol in a fixed bed reactor. Catalysts were prepared from the Na form of a commercial, pelleted X-type zeolite by ion exchange with alkali cations. Selectivity for side-chain alkylation increased when alkali hydroxide solution instead of alkali salts was used for ion exchange. High selectivity for ethylbenzene formation was achieved on zeolites in the K or Cs form containing excess alkali hydroxides. The turnover number in side-chain alkylation increases with the decreasing amount of strongly adsorbed pyridine or acetic acid per cation. © 1987 Academic Press, Inc.

INTRODUCTION

Chemical industry, because of economical considerations, presently favors toluene to benzene as a starting material for many processes (*1*). Side-chain alkylation of toluene with methanol results in styrene and/or ethylbenzene. In the production of styrene this process offers the advantage of lower raw material cost compared with the traditional Friedel–Crafts alkylation of benzene with ethene.

The side-chain alkylation of toluene proceeds on catalysts with basic properties such as basic oxides (*2*) as well as X and Y zeolites exchanged with alkali cations (*3, 4*). Over zeolites exchanged with alkali cations the selectivity for side-chain alkylation against benzene ring alkylation increases in the sequence of size of the alkali cation (Li < Na < K < Rb < Cs) (*3–6*). X zeolites were found to be more effective catalysts than the corresponding Y zeolites (*7*). According to Itoh *et al.* (*8, 9*) both basic and weak acid sites on the zeolite are required for side-chain alkylation.

Sidorenko and Galich (*5*) suggested that in side-chain alkylation of toluene with methanol styrene is formed by the reaction of toluene and formaldehyde produced by the dehydrogenation of methanol, and then part of the styrene is hydrogenated to ethylbenzene with H_2 produced in methanol dehydrogenation.

Selectivity for styrene formation can be improved by directing the decomposition of methanol toward the desired dehydrogenation. According to Sefcik (*6*) and to Unland and Barker (*7*) this can be achieved by the postexchange treatment of Cs–X zeolite with borates. This treatment leads to a higher styrene/ethylbenzene ratio by reducing the number or the strength of the excess basic sites of the catalyst. Slightly stronger acid sites in Rb–X zeolite were produced by Itoh *et al.* (*9*) by introducing a small amount of Li^+ ions. This way the undesired decomposition of formaldehyde formed from methanol was hindered.

An opposite effect, an increase in the ethylbenzene/styrene ratio, is obtained on Cs–X and Cs, B–X zeolite catalysts by having Cu and Ag promoters (*10*). On the promoted catalysts the yield in side-chain alkylation increased using hydrogen as a carrier gas.

Our results indicate that efficiency of X zeolite catalyst in side-chain alkylation is

0021-9517/87 $3.00

increased by occluded KOH. Correlation was found between the basic and the acidic characters of the catalysts and their activity and selectivity in side-chain alkylation of toluene.

EXPERIMENTAL

Preparation of the catalysts. Catalysts were prepared by ion exchange of commercial X-type zeolite (Strem Chemicals, Inc.) in the form of $\frac{1}{16}$-in. pellets. Twenty-grams of zeolite precalcined at 673 K for 2 h was treated in a column at 343 K by recirculating 0.5 *N* aqueous solution of the corresponding alkali compound as specified in Table 1. Ion exchange was carried out in three subsequent steps, twice with 600 cm^3 and a third time with 800 cm^3 solution, for 3 h each. The zeolites were then treated in three different ways:

(a) filtered without washing (f),

(b) washed with 3 × 800 cm^3 of bidistilled water at room temperature (w), and

(c) washed with 500 cm^3 0.5 *N* aqueous KOH solution at room temperature for 3 h and then filtered without washing with water (x).

TABLE 1

Preparation and Cation Content of the Various Catalysts

Catalyst designation	Zeolite content[a]	Solution used for ion exchange	Cation content[b]		
			Na^+	K^+	Cs^+
Na–X[c]	70	—	4.8	0.1	—
Na–X(Cl)w	75	NaCl	4.9	0.1	—
Na–X(OH)w	92	NaOH	5.7	0.1	—
Na–X(OH)f		NaOH	5.8	0.1	—
K–X(Cl)w		KCl	0.9	3.6	—
K–X(Cl)x		KCl	0.8	4.1	—
K–X(NO_3)w		KNO_3	0.9	3.6	—
K–X(NO_3)x		KNO_3	0.9	3.7	—
K–X(OH)w		KOH	1.5	3.2	—
K–X(OH)f		KOH	1.3	3.6	—
K–X(OH)x		KOH	1.4	3.6	—
Cs–X(Cl)w		CsCl	1.9	0.1	1.9
Cs–X(OH)w		CsOH	1.7	0.1	2.0
Cs–X(OH)f		CsOH	1.7	0.1	2.2

Note. For definitions of w, f and x, see text.

[a] Mass percentage, based on X-ray diffraction measurements.

[b] In 10^{-3} mol/$g_{cat.}$

[c] Initial sample; $Fe^{3+}/Me^+ = 9 \times 10^{-3}$ mol/mol.

All catalysts were dried at 373 K for 5 h. The characteristics of the catalysts used in this study are collected in Table 1.

Alkylation experiments. Toluene and methanol were of 97 and 99.5% purity, respectively. Experiments were carried out in a fixed bed flow reactor made of Pyrex glass. The upper 40-cm-long part of the reactor filled with glass beads was used as evaporator and mixer. Before reaction, catalysts were activated or regenerated in a flow of oxygen at 773 K for 2.5 h and then cooled to the reaction temperature in a flow of high-purity nitrogen. Nitrogen served as carrier gas as well. A mixture of toluene and methanol was fed continuously into the nitrogen stream by a micropump. The effluents from the reactor were cooled to 273 K and the condensate collected in a trap was analyzed periodically.

Reaction conditions were the same in each experiment reported here: reaction temperature = 698 K, toluene/methanol = 5.0 mol/mol, space time (W/F) = 6.0 × 10^5 $g_{cat.}$ s mol^{-1}, where

$$W/F = \frac{\text{mass of the catalyst (g)}}{\text{feed rate of (toluene + methanol) (mol s}^{-1})}. \quad [1]$$

Samples were analyzed by gas chromatography using a 3-m-long column with Benton-34/Sp-1200 on Chromosorb W, and a flame ionization detector. For quantitative analysis, benzene was used as internal standard. The yield of product was calculated as follows:

$$Y\ (\text{mol}\%) = \frac{\text{moles of products}}{\text{moles of methanol fed}} \times 100. \quad [2]$$

X-ray diffraction studies. X-ray powder diffraction measurements were carried out by a Philips PW 1050-type diffractometer using Ni-filtered Cu$K\alpha$ radiation.

IR spectroscopic measurements. Self-supporting wafers of about 10 mg cm^{-2} "thickness" were pressed from a fine powder of the catalysts, mounted on a gold rack, and positioned in an IR cell between CaF_2 windows. Turning the cell upside down one could move the catalyst rack assembly to the other end of the vacuum-tight cell. This section of the cell could be heated by an electric furnace. Wafers in the cell were evacuated at 673 K for 1 h, then exposed at 298 K to pyridine vapor at 2.4 kPa for 10 min, and evacuated at 423 K for 20 min. The infrared spectra were recorded with a Perkin–Elmer 577 double-beam grating spectrometer at room temperature in the frequency range of 1300–1700 cm^{-1}.

Pyridine and acetic acid adsorption measurements. A flow gravimetric technique was used to measure the adsorption of pyridine and acetic acid. Helium carrier gas was purified in a trap containing active charcoal and cooled with liquid nitrogen. In order to prevent the reaction of adsorbate with the electrobalance (Sartorius, Type 4102) a positive flow of high-purity nitrogen was maintained through the balance case; back-diffusion of adsorptive from the hang-down tube was avoided by means of a long, narrow tube carrying the N_2 from the balance case to the top of the hang-down tube. Pure helium or helium saturated with the adsorptive at 293 K entered from the bottom of the tube, went past the catalyst in a quartz bucket, and was led out together with the N_2 purge at the top of the hang-down tube. Pure helium flow was employed during activation and during the desorption experiment. The flow rate of helium was 160 cm^3 min^{-1} and that of nitrogen was 30 cm^3 min^{-1}. Two hundred milligrams of catalyst was calcined at 673 K until constant weight was reached, and then it was cooled to 553 K. Adsorption and desorption measurements were carried out at this temperature.

The weight of adsorbed pyridine or acetic acid was determined as a function of time. Plots for each catalyst were of similar character (Fig. 1). The weight gain of the sample at the stage when weight did not change with time was taken as the value of total adsorption (given as "a" in Fig. 1). When saturation of the sample in helium–adsorptive mixture was reached, the sample was purged with pure helium in order to determine the amount of adsorbate strongly bound (given as "b" in Fig. 1).

CO_2 adsorption capacity measurements. At 198 K, up to pressures of about 10^5 Pa, carbon dioxide is bound practically exclusively in the pores of the zeolite (*11*). The CO_2 adsorption capacity of catalysts is therefore proportional to their zeolite content. Carbon dioxide adsorption isotherms were determined in a conventional BET volumetric system at the temperature of dry ice acetone. The samples were pretreated by evacuation at 673 K for 10 h.

RESULTS

In alkylation experiments, the yield changed with time on stream (Fig. 2). In most of the experiments with fresh catalysts the yield increased in the first 2–3 h and then decreased. When different catalysts were compared, the yields averaged for the first 5 h of experiments were taken into account.

The yield of xylenes, in agreement with previous findings, decreased in the catalyst

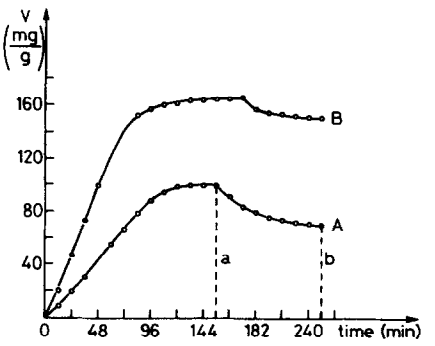

FIG. 1. Pyridine (A) and acetic acid (B) adsorption/desorption at 553 K on Na–X(Cl)w. (a) Total amount of adsorbed material; (b) amount of strongly adsorbed material.

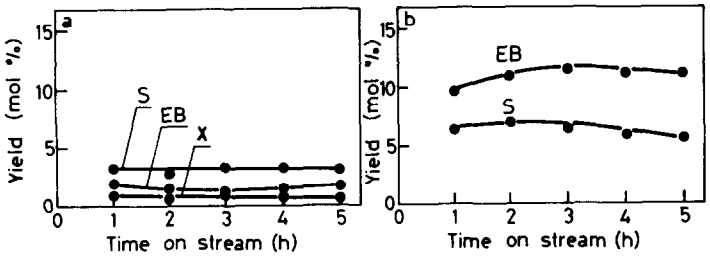

FIG. 2. Change of yields with time on stream for (a) Cs–X(Cl)w, (b) Cs–X(OH)w. (S, styrene; EB, ethylbenzene; X, Σxylenes)

sequence Na–X(Cl)w > K–X(Cl)w > Cs–X(Cl)w; the reverse tendency was found for the yield of ethylbenzene and styrene. No side-chain alkylation was observed on Na–X(Cl)w, but ethylbenzene and styrene were produced on K–X(Cl)w and Cs–X(Cl)w (Fig. 3a). The decrease in benzene ring alkylation is more significant than the increase in side-chain alkylation; therefore the total yield of C_8 hydrocarbons decreased in the sequence of catalysts containing Na > K > Cs. It should be noted that even over Cs–X(Cl)w the yield of xylenes is not negligible in relation to the yield of styrene and ethylbenzene.

Higher selectivities for side-chain alkylation were obtained on catalysts ion exchanged with alkali hydroxide solution than on those ion exchanged with alkali chloride solution (Fig. 3b). Formation of ethylbenzene was already observed on Na–X(OH)w. The selectivity for side-chain alkylation was much higher on K–X(OH)w and reached 100% on Cs–X(OH)w. The total yield of C_8 aromatics showed a minimum value on K–X(OH)w.

An even more pronounced change in selectivity toward side-chain alkylation was observed when zeolites obtained by ion exchange with alkali hydroxides were filtered without washing with water (Fig. 3c). Both over K–X(OH)f and Cs–X(OH)f only side-chain and no benzene-ring alkylations were observed. The total yield of C_8 aromatics increased in the sequence Na–X(OH)f < K–X(OH)f < Cs–X(OH)f. The

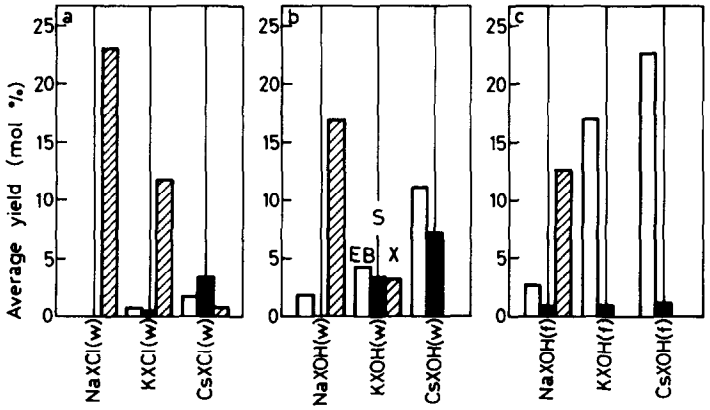

FIG. 3. Activity of catalysts obtained by ion exchange with (a) alkali chlorides, (b) alkali hydroxides, (c) alkali hydroxides without washing with water. (S, styrene; EB, ethylbenzene; X, Σxylenes)

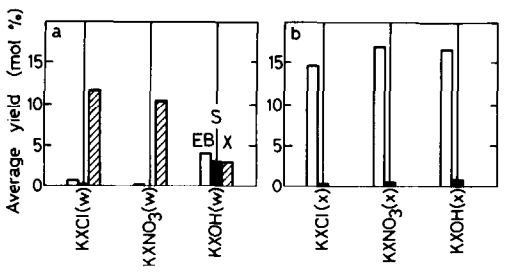

FIG. 4. Activity of catalysts prepared by ion exchange with different potassium compounds and (a) washed with water, (b) washed with 0.5 *N* aqueous KOH solution. (S, styrene; EB, ethylbenzene; X, Σxylenes)

ratio of styrene/ethylbenzene is significantly lower than that in the products obtained on catalysts exchanged by alkali hydroxide and washed with water.

Catalysts ion exchanged with solutions of different potassium compounds were treated with KOH. The effect of this treatment on activity and selectivity of the catalysts can be seen in Fig. 4. The selectivity for side-chain alkylation is higher on K–X(OH)w than on K–X(Cl)w and K–X(NO_3)w (Fig. 4a), but it is still quite small. Washing the catalysts with KOH solution after ion exchange results in a perfect selectivity for side-chain alkylation and in higher yields of C_8 aromatics (Fig. 4b). Similar behavior of the samples points to the decisive role of occluded KOH.

Experiments were carried out over catalyst K–X(OH)f washed with water to different extents (Fig. 5). Catalysts K–X(OH)w1–w3 were obtained by washing K–X(OH)f (10 g) after ion exchange with 300 cm^3 of water one to three times for 3 min each; K–X(OH)w4 was obtained by washing until disappearance of K^+ ions in the washing water. As can be seen, side-chain alkylation was gradually replaced by benzene-ring alkylation as the extent of washing increased. There was no difference in the activity of catalysts K–X(OH)w3 and K–X(OH)w on the one hand and K–X(OH)w4 and K–X(Cl)w on the other. From this it follows that the low selectivity of catalysts in side-chain alkylation can be restored by effective removal of excess KOH.

The results reported so far were obtained over fresh catalysts. Activity/selectivity of different catalysts varied in different ways upon regeneration. For example, over catalyst K–X(OH)f, the yield of ethylbenzene decreased, but that of styrene increased with the increasing number of regenerations (Fig. 6). Over catalyst Cs–X(OH)w, however, the yield of styrene reached an almost constant level, while that of ethylbenzene gradually decreased with regeneration (Fig. 7). Consequently, the styrene/ethylbenzene ratio increased with each regeneration over both catalysts. In the case of K–X(OH)f, this ratio increased with time on stream as well, but never reached the ratio obtained on Cs–X(OH)w.

The infrared spectra of pyridine adsorbed on ion-exchanged zeolites (Fig. 8) failed to show an unambiguous correlation between acidity and catalytic activity of the catalysts. The band at 1545 cm^{-1}, characteristic of pyridine adsorbed on Brønsted acid sites, appeared only on catalysts obtained in exchange with alkali chlorides and nitrates (curve a). Over catalysts prepared in ion exchange with alkali hydroxides, although they were active in benzene-ring alkylation, this band was not observed (curve b). It was missing in the spectra of pyridine adsorbed on catalysts with excess

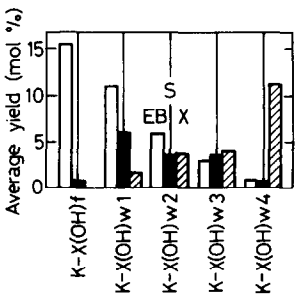

FIG. 5. Activity of catalyst prepared by ion exchange with KOH. Effect of washing with water (see text). (S, styrene; EB, ethylbenzene; X, Σxylenes)

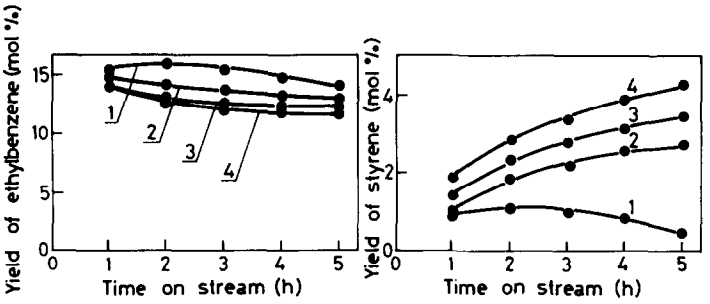

FIG. 6. Change of yields with time on stream over fresh (curve 1) and one to three times regenerated (curves 2–4) catalyst K–X(OH)f.

alkali hydroxide as well, but a new band appeared at 1375 cm^{-1} (curve c). This band was observed in spectra recorded before adsorption of pyridine and in the spectrum of KOH in KBr matrix as well.

Isotherms for adsorption of CO_2 on different catalysts can be seen in Fig. 9. The saturation capacities of adsorption on Na–X(Cl)w and K–X(Cl)w are almost the same (curves a and b), but that of Cs–X(Cl)w is noticeably lower (curve c). There is no significant difference in the adsorption capacities of catalysts prepared by alkali chloride and by alkali hydroxide solutions (compare curves b and d as well as c and e). The adsorption capacity of catalyst K–X(OH)x is decreased due to effect of excess KOH (curve f). No structural changes are responsible for the lower adsorption capacity of Cs–X(Cl)w, because after ion exchange again with NaCl, the adsorption capacity of the catalyst was the same as that of Na–X(Cl)w (curve g).

X-ray powder diffractograms are shown in Fig. 10. Peak intensities decrease in the sequence of pure Na–X powder (a) > Na–X(OH)w (b) > Na–X(Cl)w (c) > K–X(Cl)w (d) > K–X(Cl)x (e) > Cs–X(Cl)w (f). Each spectrum is characteristic for X zeolite. The diffractogram of the catalyst obtained from Cs–X(Cl)w by ion exchange with NaCl solution is almost identical with that obtained on Na–X(Cl)w (compare c and g).

Adsorbed amounts of pyridine and acetic acid on different catalysts are given in Table 2. The amounts of both the total and strongly adsorbed pyridine and acetic acid decrease in the sequence Na–X(Cl)w > K–X(Cl)w > Cs–X(Cl)w.

Pyridine adsorption measurements were carried out under conditions identical to those above on K–X(OH) catalyst washed

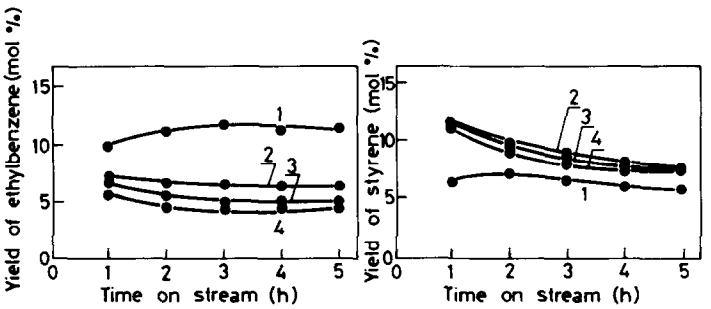

FIG. 7. Change of yields with time on stream over fresh (curve 1) and one to three times regenerated catalyst Cs–X(OH)w.

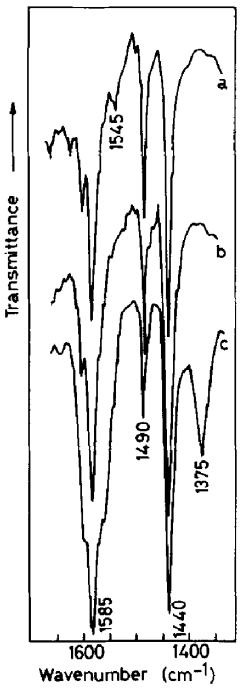

FIG. 8. Infrared spectra of pyridine adsorbed on catalysts (a) K–X(NO_3)w, (b) K–X(OH)w, (c) K–X(NO_3)x.

TABLE 2

Amount of Total and Strongly Adsorbed Pyridine and Acetic Acid on Various Catalysts

Catalysts	Pyridine adsorbed ($mg/g_{cat.}$)		Acetic acid adsorbed ($mg/g_{cat.}$)	
	Total	Strongly	Total	Strongly
Na–X(Cl)w	99.4	69.0	165.5	154.9
K–X(Cl)w	79.6	45.6	125.7	121.4
Cs–X(Cl)w	61.7	29.5	99.4	91.4

to different extents. The results can be seen in Table 3. Independent of the extent of washing, the total amount of adsorbed pyridine remained practically constant. The amount of strongly adsorbed pyridine, however, increased with the increasing extent of washing.

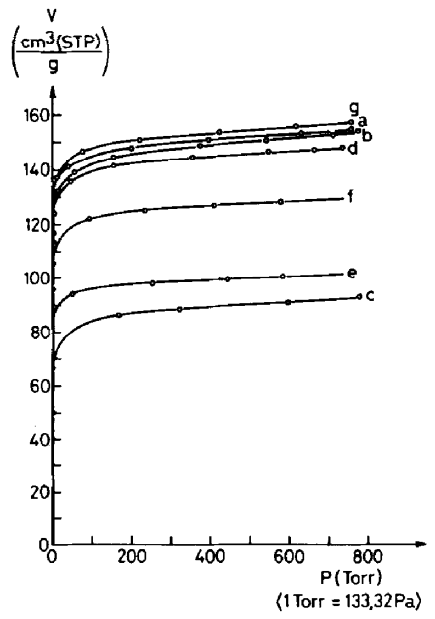

FIG. 9. CO_2 adsorption isotherms at 195 K on (a) Na–X(Cl)w, (b) K–X(Cl)w, (c) Cs–X(Cl)w, (d) K–X(OH)w, (e) Cs–X(OH)w, (f) K–X(OH)x, (g) Cs–X(Cl)w reexchanged for Na.

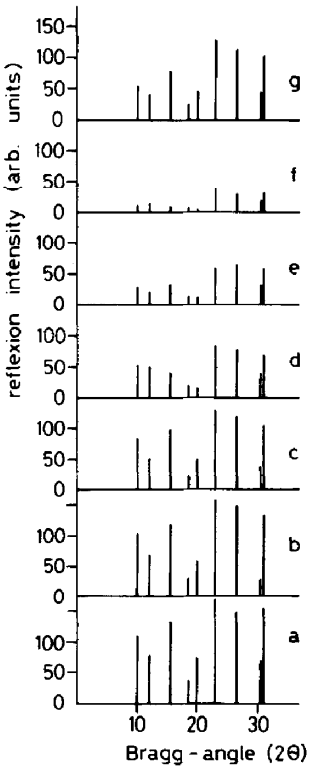

FIG. 10. X-ray powder diffractograms determined on (a) Na–X without binder, (b) Na–X(OH)w, (c) Na–X(Cl)w, (d) K–X(Cl)w, (e) K–X(Cl)x, (f) Cs–X(Cl)w, (g) Cs–X(Cl)w reexchanged for Na.

TABLE 3

Amount of Total and Strongly Adsorbed Pyridine on K–X(OH) Catalyst Washed to Different Extents

Catalysts	Pyridine adsorbed ($mg/g_{cat.}$)	
	Total	Strongly
K–X(OH)w1	79.5	21.2
K–X(OH)w2	80.2	25.1
K–X(OH)w3	81.3	31.8
K–X(OH)w4	80.8	38.2

DISCUSSION

Quantum-chemical calculations have shown that the presence of basic sites is indispensable to the side-chain alkylation of toluene (*8*). Furthermore, the calculations have indicated that this reaction requires specific steric configurations of acidic and basic sites. Formaldehyde formed by the dehydrogenation of methanol attacks the methyl group of toluene adsorbed on acidic and basic sites. Alkali-cation-exchanged X and Y zeolites possess acidic and basic sites in an appropriate pore structure satisfying the steric requirements. This explains why the alkali-cation-exchanged Y and especially X zeolites are more active and selective than other catalysts in this reaction.

The increase in selectivity of catalysts in side-chain alkylation in the sequence of size of the cations therein has been correlated with the increasing inhibition of rotation of toluene in the zeolite cavity (*6*). The replacement of the sodium cation with larger cations prevents reactions having transition complexes larger than the space available, whereas reactions going through smaller transition complexes proceed unimpeded. The aromatic ring is already severely hindered in rotation when toluene is adsorbed on Cs–X, and therefore it is unlikely that a transition complex involving ring attack could occur. Besides steric hindrance the increase in basicity with increasing cation size must be considered as a factor improving catalytic selectivity.

In agreement with previous findings, the activity of catalysts obtained from X zeolite by ion exchange with alkali cations increased in side-chain alkylation and decreased in ring alkylation in the sequence of Na, K, and Cs forms (Fig. 3a). Selectivities for side-chain alkylation, however, were lower on the catalysts studied than those reported in the literature (*4*, *7*, *8*).

As a matter of fact there is a slight, but not negligible difference in the preparation of the catalysts used by us and that described elsewhere. Generally pure zeolite powder is ion exchanged and pressed into pellets without binder. These catalysts, however, do not have a mechanical strength sufficient for industrial application. Industrial interest initiated us to use commercial pelleted zeolite for catalyst preparation.

According to the X-ray powder diffractometric measurements (Figs. 10a and 10c) and chemical analysis, the pelleted zeolite contained approximately 30% alumina as binder. The lower selectivity in side-chain alkylation can be attributed to the remaining acidity of alumina. The increase in the peaks in X-ray diffractograms due to ion exchange with NaOH (Fig. 10b vs Fig. 10c) suggests that the binder can be partially removed by alkali hydroxide solution.

The increase in the relative alkali cation content of catalysts upon treatment with KOH solution indicated as well that the catalysts became richer in zeolite due to removal of binder (Table 1).

Using alkali hydroxide solutions for ion exchange instead of the solution of the respective salt, there is a more significant change in the acidity and selectivity of catalysts. The appearance of ethylbenzene in the products over Na–X(OH)w (Fig. 3b) indicates that basic sites were formed even on an otherwise acidic Na–X zeolite. In the infrared spectra of pyridine adsorbed on

catalysts (Fig. 8) the band at 1545 cm^{-1}, characteristic of pyridine adsorbed on Brønsted acid sites, appeared on catalyst only exchanged with alkali nitrate (curve a), but was not observed on catalyst exchanged or treated with alkali hydroxide (curves b and c).

A lower activity for alkylation on Cs–X than that on Na–X or K–X zeolites was found by Yashima *et al.* (*4*) who explained this as a result of partial destruction of catalyst crystallinity due to exchange with Cs^+. In our case the total yield of C_8 aromatics decreased in the sequence Na–X(Cl)w > K–X(Cl)w > Cs–X(Cl)w (Fig. 3a). A similar decrease in intensities of X-ray reflections was observed on the diffractograms (Figs. 10c, 10d, and 10f). The CO_2 adsorption capacities of Na–X(Cl)w and K–X(Cl)w were identical, but that of Cs–X(Cl)w was significantly lower (Figs. 9a, 9b, and 9c). From these observations it might be concluded that destruction of the zeolite structure takes place upon exchange with Cs^+. Both intensities of X-ray reflections (Fig. 10g) and CO_2 adsorption capacity (Fig. 9, curve g) of the sample prepared from Cs–X(Cl)w by back-exchange into the Na form were identical to those of the original Na–X(Cl)w. Consequently, in our case, no irreversible structural destruction occurred upon Cs ion exchange. Presumably some of the adsorption sites were blocked for CO_2 molecules by large Cs^+ ions resulting in a decrease in the adsorption capacity of Cs–X(Cl)w compared to that of the Na form. X-ray diffractograms of the different cationic forms of a given zeolite can be of different intensities, i.e., no simple correlation between crystallinity and reflection intensity exists. However, the diffractogram of the Cs zeolite indicates that the faujasite structure remained unchanged.

It can be seen in Table 2 that the amount of both the total and the strongly adsorbed pyridine and acetic acid decrease in the sequence Na–X(Cl)w > K–X(Cl)w > Cs–X(Cl)w. The total amount of adsorbed pyridine was found to be independent, within the limit of errors of the measurements, from the kind of ion exchange solution (KCl or KOH) and from the effectiveness of catalyst washing (compare data of Tables 2 and 3).

TABLE 4

Acidic Character of the Catalysts and Their Activity in Benzene-Ring Alkylation of Toluene with Methanol

Catalysts	Pyridine adsorbed[a] $\times 10^2$ (mmol $g_{cat.}^{-1}$)[b]	Activity $\times 10^5$ (mmol $g_{cat.}^{-1}$ s^{-1})[b]
Na–X(Cl)w	98.8	72.3
K–X(Cl)w	68.7	38.8
Cs–X(Cl)w	53.3	2.8

[a] Strongly adsorbed pyridine.

[b] Weight of catalyst corrected with the weight of alkali cations therein.

We assumed that the amount of strongly bound pyridine under fixed conditions (temperature and partial pressure of the adsorptive) is a function of the number and strength of acid sites only. These amounts, correlated with the corrected weights of catalysts, are given in Table 4. The corrected weight was obtained as a difference of the total weight of the catalyst and the weight of alkali cations therein; the corrected weight is proportional to the number of unit cells in a given catalyst. For comparison the activities of the catalysts in benzene ring alkylation are also shown (Table 4). The greater the number of strongly bound pyridine molecules, the higher is the activity of the catalyst in the benzene ring alkylation reaction.

In alkali-cation-exchanged zeolites the cations are Lewis acids; the base in the acid–base pair is the zeolite framework itself. The adsorbed amount of acetic acid per cation was supposed by us to measure the average base strength of one sorption site and was expected to increase in the sequence opposite to that observed for pyr-

TABLE 5

Acid–Base Properties of the Catalysts and Their Activity in Side-Chain Alkylation of Toluene with Methanol

Catalysts	Strongly adsorbed		Turnover number
	Pyridine (mol/mol$_{cation}$)	Acetic acid (mol/mol$_{cation}$)	(mol/mol$_{cation}$ s)
Na–X(Cl)w	0.19	0.57	0.0
K–X(Cl)w	0.13	0.49	2.3
Cs–X(Cl)w	0.11	0.46	14.0

idine. The number of acetic acid and pyridine molecules and the turnover numbers in side-chain alkylation, both related to the alkali cation content of catalysts, are collected in Table 5. The number of alkali cations was considered to give the number of acid and base sites. The expected correlation between the adsorption of acetic acid and the turnover number was not found. It seems probable that similarly to pyridine a weak acid like acetic acid interacts rather with the strong Lewis acid sites, i.e., with the alkali cations, than with the Lewis base zeolite framework.

Catalysts obtained by ion exchange with alkali hydroxide solution and filtered without washing with water showed significantly higher selectivity in side-chain alkylation than those prepared by the conventional method (Fig. 3c). Similar high selectivity was achieved when catalysts prepared by ion exchange with alkali salts were treated with KOH solution (Fig. 4). The observation that the selectivity for ring alkylation increased by increasing the extent of washing out of K–X(OH)f (Fig. 5) shows that improvement of catalytic performances resulted from occluded KOH rather than from structural changes.

As can be seen in Table 1, the differences in the cation content of the catalysts filtered only, or washed with water or KOH solution, are within the error limits of the analytical measurements. Considering the pore volume of the zeolite and the concentration of the KOH solution, the ratio of cations occluded to cations exchanged is of the order of magnitude of $\frac{1}{100}$, i.e., within the limit of analytical error.

The presence of "occluded" KOH can be revealed in infrared spectra. On the spectrum of the catalyst with excess alkali hydroxide a new band appeared at 1370 cm^{-1} (Fig. 8, spectrum c). This band can be observed in the spectrum of KOH in KBr matrix as well.

As in the case of catalysts containing Cs^+, both CO_2 adsorption capacity (Fig. 9, curve f) and the reflection intensities in X-ray diffractogram (Fig. 10e) decrease due to the effect of occluded KOH. As can be seen in Table 3, pyridine adsorbed strongly increased with the increasing extent of KOH removal from K–X(OH)f catalyst. In this context a fairly good correlation can be found between the amount of adsorbed pyridine and the activity of the catalyst in ring alkylation.

Selectivity for side-chain alkylation is influenced positively by relatively small amounts of occluded alkali hydroxides; however, concomitantly the ratio of styrene/ethylbenzene decreases significantly (cf. Figs. 3b and 3c, as well as Fig. 4). As with Cu and Ag promoters (*10*), alkali hydroxides deposited on the zeolite surface act as sites for hydrogenation.

Interestingly enough, regeneration of catalysts with oxygen suppressed their hydrogenation activity (Figs. 6 and 7). The yield of ethylbenzene decreased over both K–X(OH)f and Cs–X(OH)w with the increasing number of reaction–regeneration cycles. Unfortunately, over Cs–X(OH)w, where the ratio styrene/ethylbenzene is higher than that over K–X(OH)f, the deactivation of the catalyst, presumably due to coke formation, is more significant.

In conclusion it can be stated that high selectivity for ethylbenzene can be achieved in alkylation of toluene with methanol on catalysts prepared from commercial pelleted X zeolite by ion exchange with Cs^+ or even K^+ cations, when the catalysts contain occluded alkali hydroxides. The

yield for ethylbenzene decreases and that for styrene increases upon regeneration with oxygen.

REFERENCES

1. Brownstein, A. M., *in* "Catalysis of Organic Reactions" (W. R. Moser, Ed.), p. 3. Dekker, New York, 1981.
2. Tanabe, K., Takahashi, O., and Hattori, H., *React. Kinet. Catal. Lett.* **7,** 347 (1977).
3. Sidorenko, Y. N., Galich, P. N., Gutyrya, V. S., Ilin, V. G., and Neimark, I. E., *Dokl. Akad. Nauk. SSSR* **173,** 132 (1967).
4. Yashima, T., Sato, K., Hayasaka, T., and Hara, N., *J. Catal.* **26,** 303 (1972).
5. Sidorenko, Y. N., and Galich, P. N., *Dokl. Akad. Nauk. SSSR* **174,** 1234 (1968).
6. Sefcik, M. D., *J. Amer. Chem. Soc.* **101,** 2164 (1979).
7. Unland, M. L., and Barker, G. E., *in* "Catalysis of Organic Reactions" (W. R. Moser, Ed.), p. 51. Dekker, New York, 1981.
8. Itoh, H., Miyamoto, A., and Murakami, Y., *J. Catal.* **64,** 284 (1980).
9. Itoh, H., Hattori, T., Suzuki, K., and Murakami, Y., *J. Catal.* **79,** 21 (1983).
10. Lacroix, C., Deluzarche, A., Kienneman, A., and Boyer, A., *Zeolites* **4,** 109 (1984).
11. Valyon, J., Papp, J., and Kalló, D., *Acta Chim. Acad. Sci. Hung.* **106,** 131 (1981).